COMPDYN 2013
4th ECCOMAS Thematic Conference on
Computational Methods in Structural Dynamics and Earthquake Engineering
M. Papadrakakis, V. Papadopoulos, V. Plevris (eds.)
Kos Island, Greece, 12–14 June 2013

INFLUENCE OF SOIL-STRUCTURE INTERACTION ON ISOLATED BUILDINGS FOR SF6 GAS-INSULATED SUBSTATIONS

L. E. Pérez Rocha[1], J. Avilés López[2], A. Tena Colunga[3], C. Cordero Macías[4]

[1] Instituto de Investigaciones Eléctricas
Cuernavaca 62490, Morelos, México
e-mail: lepr@iie.org.mx

[2] Instituto Mexicano de Tecnología del Agua
Jiutepec 62550, Morelos, México
e-mail: javiles@tlaloc.imta.mx

[3] Universidad Autónoma Metropolitana
Azcapotzalco 02200, Distrito Federal, México
e-mail: atc@correo.azc.uam.mx

[4] Comisión Federal de Electricidad
Cuauhtémoc 06500, Distrito Federal, México
e-mail: cuauhtemoc.cordero@cfe.gob.mx

Keywords: Soil-structure interaction, seismic isolation, floor spectra.

Abstract. *For earthquake excitation, base isolators have been successfully used in building structures on firm ground. However, the use of these devices in buildings on soft soil for SF6 gas-insulated substations introduces the following concerns: a) the frequency and damping characteristics of the fixed-base structure may change significantly by the combined effects of soil-structure interaction (SSI) and the base isolation device; and b) very large displacements may result because of the translation and rocking of the foundation. In this paper, the effects of SSI on the seismic response of a base-isolated MDOF system are investigated. Both kinematic and inertial effects are considered. The effective input motions (translation and rocking) for an embedded foundation are computed with the averaging Iguchi's method. The soil is replaced by frequency-dependent elastic springs and viscous dampers computed with a finite layer method. The SSI analysis is performed in the frequency domain with the complex frequency method. Numerical results, including floor response spectra of acceleration and displacement, are computed for SSI conditions prevailing in Mexico City, where SF6 gas-insulated substations are being projected. The base isolation device must be capable of accommodating displacements associated with different performance levels.*

1 INTRODUCTION

The dynamic soil-structure interaction (SSI) is a set of kinematic and inertial effects in the structure and the soil as a result of the deformability of the latter before seismic excitation [1]. The SSI modifies relevant dynamic properties that the structure had in the fixed base condition, as well as the ground motion characteristics around the foundation. Elongation of the fundamental period and increment of modal damping are due to inertial interaction. Besides, kinematic interaction reduces translational components (filtering high frequency) but also generates rotational components (rocking and torsion).

In the conventional approach of design free field surface spectra are often used. However, these spectra may not be representative of the motion of foundation. There are two neglected effects: a) the diffraction of incident waves by the foundation (kinematics interaction) and b) the effect on the soil of the inertia forces generated in the structure and foundation (inertial interaction). It is better to determine floor response spectra, computed with the actual motion of foundation that results from a complete SSI analysis. These site spectra with SSI are specific for the soil-structure system and are applied as free-field spectra, assuming fixed base structure.

To evaluate the feasibility of using seismic isolation in buildings for encapsulated substations in the Valley of Mexico, it is necessary to consider the effects of SSI in the model of analysis. To a first approximation, we considered fixed base models and free field excitations. Now we analyze the effects of SSI on the effectiveness of the insulation system, which aims to reduce the seismic forces when the effective flexibility and damping of support are increased.

SSI analysis is based on the principle of superposition in three steps [2], namely:

1. *Kinematic interaction:* Determination of foundation motion supposed rigid and massless under seismic waves propagation.
2. *Impedance Functions:* Computation of dynamic stiffness of the foundation supposed rigid and massless, which are defined by forces and moments required to produce unit harmonic displacements and rotations, respectively.
3. *Inertial interaction:* Determination of structure response supported on springs and dashpots in step 2 and subjected to the effective motion at its base from step 1.

2 FREE FIELD RESPONSE ANALYSIS

The free field response in a soil deposit can be computed with the one-dimensional model of propagation of shear waves [3]. This model allows to consider effects related to soil stratification, flexibility of the base and nonlinearity of materials. The seismic excitation is given in terms of a uniform hazard spectrum (UHS) at rock.

2.1 Design earthquake

The rock UHSs are constructed by the weighted contribution of all possible events, namely subduction earthquakes, normal faulting, and local intraplate. The weighting factor is given mainly by the seismicity of the various sources and their distance to the Valley of Mexico. Rock UHS (5% damping) for return period of 475 years, that is the basis of regulatory design spectra [4] was used in this study. It will be called as design earthquake.

Known the target response spectrum, synthetic accelerograms can be simulated. They are representative of the ground motion to the basement level. From these accelerograms, it is possible to compute the free field response at the surface. Specifically, a simulation method that accomplishes with prescribed spectral amplitudes is used. The principle of the method is to build transient signals whose response spectra iteratively fit the target response spectrum. Figs 1 and 2 show the synthetic accelerograms as well as the achieved compatibility with the objective response spectra. These movements are artificial but conservative, since the calculated spectral ordinates are adjusted in all vibration periods and not only in the characteristic periods of ground motion. These spectra exhibit two peaks in vibration periods near 0.25 and 1 s. The first is associated with near-field earthquakes (local and intraplate normal faulting) and the second far-field earthquakes (subduction).

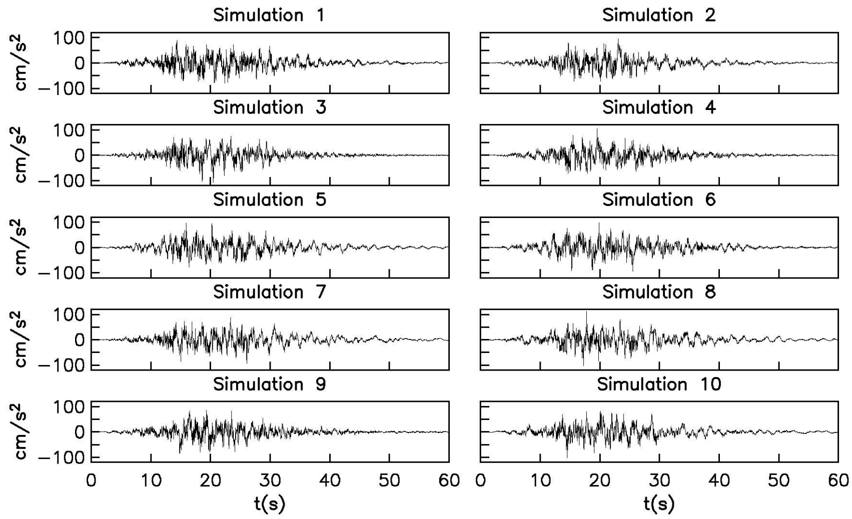

Fig. 1. Synthetic accelerograms on rock ($\ddot{x}_g$).

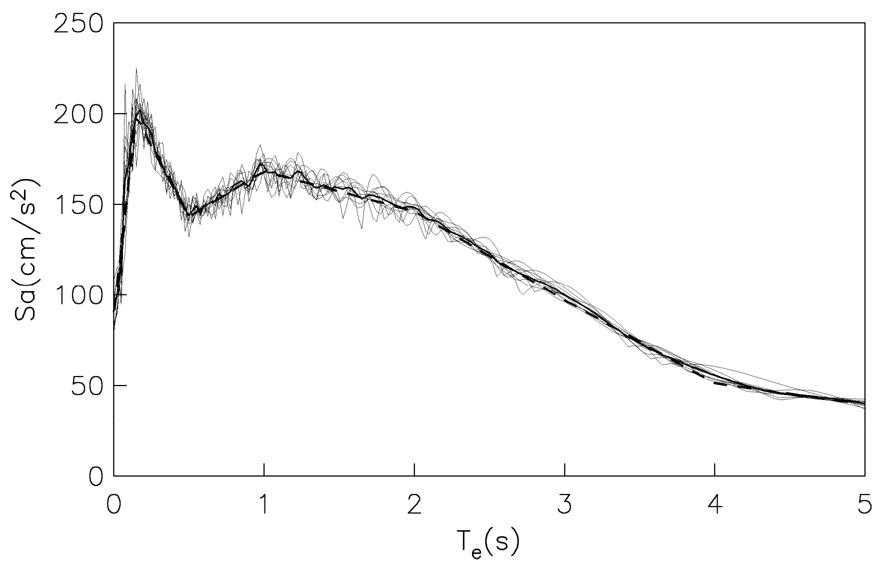

Fig. 2. Response spectra simulations (thin lines), average response spectrum (continuous thick line) and target uniform hazard spectrum (thick dashed line).

2.2 Stratigraphic model

For the specific site, called Narvarte, subsurface data are scarce. To account for the uncertainty in the data, random possible realization of the stratigraphic profile were generated, regarding the dominant period T_s and the depth to the basement H_s specified in regulatory seismic zoning maps [5]. For this site, the period is near 1 s. and the depth of the basement ic near 40 m. The effective velocity of the site is obtained as $V_s = 4H_s/T_s$. Estimated basement shear waves velocity V_r was such that the resonant response of the site, obtained with analytical transfer functions (stratigraphic model), was similar to that obtained with empirical transfer function (spectral ratios). For each simulation of the stratigraphic profile, free field response was calculated assuming vertical propagation of shear waves.

During intense earthquakes, soils may have nonlinear behavior in their dynamic properties. To account for the degradation of stiffness and increment of damping that occurs during great deformations of the soil, the equivalent linear method [6] is applied. This establishes an iterative linear analysis corrected dynamic parameters, which stops until achieve a desired convergence.

2.3 Free field spectra

The shape of the response spectra is strongly influenced by the period of the site. The spectra in free field surface reflect exclusively the amplification effects due to local soil conditions. For 5% damping, Fig. 3 shows the specific site response spectra, corresponding to the design earthquake.

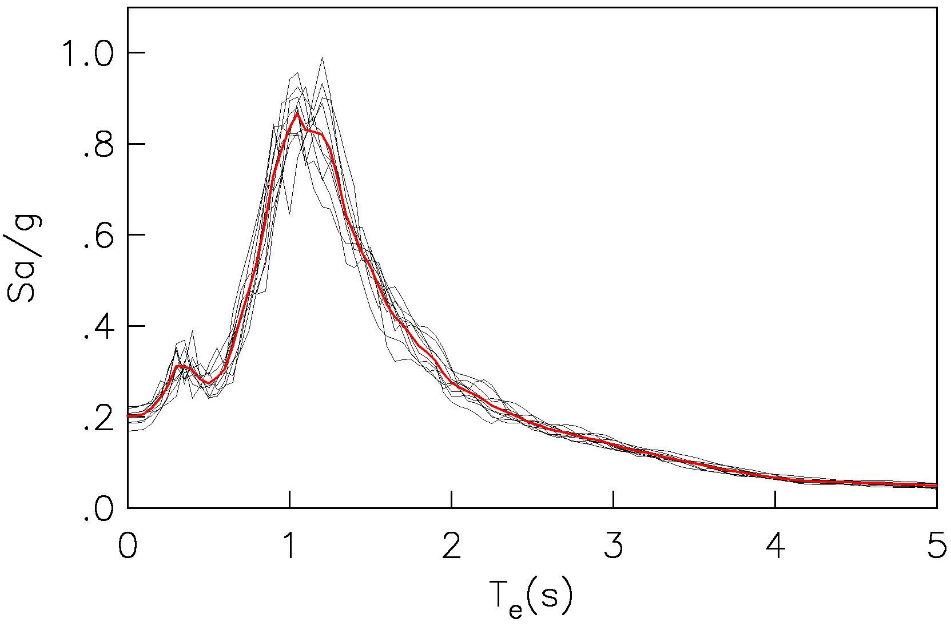

Fig. 3. Response spectra of simulations (thin black lines) and average response spectrum (thick red line), for design earthquake at Narvarte site.

3 EFFECTIVE EXCITATION AT THE BASE

Effective excitation at the base represents the input motion which results from superposing the free field with the field diffracted by the foundation. It is an artificial motion because is obtained by ignoring both the structure and the foundation masses. To calculate it is necessary to solve a complex problem of diffraction waves, hardly to model with commercial computer programs. In practical applications, the effective excitation at the base is calculated with the method of Iguchi [7]. According to this approximation method, the input motion is obtained by a weighted average of displacement and free field stresses around the foundation.

3.1 Normalized input motion

Transfer functions $H_x = \ddot{x}_b / \ddot{x}_g$ and $H_\theta = \ddot{\theta}_b / \ddot{x}_g$ were computed for an embedded foundation in a soil deposit under vertical incidence of shear waves. Damping ratios $\zeta_s = 5\%$ for soil and $\zeta_r = 3\%$ for the basement were used. These functions relate the amplitudes of the input motions (translation and rotation) with the amplitude of the free-field motion. Input motions, as dynamic stiffness are dimensionless function of frequency

$$\eta_m = \frac{\omega r_m}{V_s} \tag{1}$$

where r_m is the radius of a circle equivalent to the supporting surface of foundation with equal area and moment of inertia of that surface, ie:

$$r_x = \left(A/\pi\right)^{1/2} \tag{2}$$

$$r_\theta = \left(4I/\pi\right)^{1/4} \tag{3}$$

where A is the surface area of the foundation and I the corresponding moment of inertia respect to the axial axis of rotation, perpendicular to the direction of analysis.

4 SOIL SPRINGS AND DASHPOTS

Dynamic stiffness of foundation are complex quantities dependent of the frequency excitation. Real part expresses stiffness and inertia of the soil, while the imaginary part expresses material and geometric damping. Physically represent linear springs and viscous dashpots that replace the supporting soil.

4.1 Dynamic stiffness representation

The dynamic stiffness for any mode of vibration of the foundation ($m = h, r, hr$) is often expressed as [8]

$$\widetilde{K}_m(\eta_m) = K_m^o[k_m(\eta_m) + i\,\eta_m c_m(\eta_m)](1 + i2\zeta_s) \tag{4}$$

where K_m^o is the static stiffness, k_m and c_m are the impedance coefficients and ζ_s is ground hysteretic damping. If K_m represents a linear spring and C_m a viscous damper, the dynamic stiffness is alternatively defined by expression [8]

$$\widetilde{K}_m(\omega) = K_m(\omega) + i\omega C_m(\omega) \tag{5}$$

Therefore, the spring and dashpot are associated with the static stiffness and impedance coefficients by the following expressions:

$$K_m = K_m^o(k_m - 2\zeta_s \eta_m c_m) \tag{6}$$

$$\omega C_m = K_m^o(\eta_m c_m + 2\zeta_s k_m) \tag{7}$$

The spring K_m expresses not only rigidity but also inertia of the soil; dependence on frequency is due to the influence it has on the inertia. Furthermore, the damper C_m expresses material and geometric damping of the soil, the first is due to hysteretic behavior and the second to wave radiation.

Static stiffnesses K_h^o, K_r^o and $K_{hr}^o = K_{rh}^o$, as well as stiffness coefficients k_h, k_r and $k_{hr} = k_{rh}$ and damping coefficients c_h, c_r and $c_{hr} = c_{rh}$ were calculated by using a finite layer method [9] implemented in the computer program SUPELM [10]

5 SOIL-STRUCTURE INTERACTION ANALYSIS

Two approaches are commonly used to evaluate the effects of SSI. The first is to modify the dynamic properties of the original structure and evaluate the response of the modified structure subject to free-field motion. The second is to modify the free-field motion and evaluate the response of the original structure subjected to the motion modified by the foundation. The first approach is useful to consider the effects of SSI only in the fundamental mode of vibration, while the second approach is used to determine floor spectra applicable to all modes of the structure. In this work we adopt the second approach.

5.1 System Modeling

Fig. 4 (left) illustrates the model for the analysis of SSI in buildings with seismic isolation. For each direction of analysis, the structure is modeled as a shear beam with 4 degrees of freedom in horizontal translation and the foundation as a rigid block with two degrees of freedom, one in horizontal translation and the other in rotation. Additionally the deformation of the isolator is considered, which is modeled as a spring and dashpot in the interface between the superstructure and the substructure support. The soil is modeled with spring and dashpots that depend on the excitation frequency, although just the springs are shown, parallely also dashpots exist.

Because the dampings of soil and isolator are significantly higher than the one of the structure and therefore not proportional to its mass and stiffness, the system lacks classical modes of vibration, not allowing to perform a conventional modal superposition analysis.

The free-field motion $\ddot{x}_g$ on the surface becomes an effective excitation in the base, whose translational $\ddot{x}_b$ and rotational $\ddot{\theta}_b$ components depend on the characteristics of the foundation and the soil, as well as on the nature of the seismic excitation. For vertical incidence of shear waves, the torsional component does not exist.

5.2 Equations of Motion

With reference to Fig. 4 (right), the degrees of freedom of the system are the displacements x_1, x_2, x_3, x_4 of the structure relative to its base, the deformation x_o of the isolator and the translation x_c and the rotation θ_c of the foundation relative to the ground. Given a ground motion with translational x_b and rotational θ_b components, the equations of motion can be obtained from the kinetic energy T and the potential energy V of system. Considering first the undamped system (conservative), these energies are given by

$$\begin{aligned} T = &\frac{1}{2}M_c(\dot{x}_b+\dot{x}_c)^2 + \frac{1}{2}J_c(\dot{\theta}_b+\dot{\theta}_c)^2 + \frac{1}{2}M_o(\dot{x}_b+\dot{x}_c+h_o(\dot{\theta}_b+\dot{\theta}_c)+\dot{x}_o)^2 \\ &+\frac{1}{2}M_1(\dot{x}_b+\dot{x}_c+h_1(\dot{\theta}_b+\dot{\theta}_c)+\dot{x}_o+\dot{x}_1)^2 + \frac{1}{2}M_2(\dot{x}_b+\dot{x}_c+h_2(\dot{\theta}_b+\dot{\theta}_c)+\dot{x}_o+\dot{x}_2)^2 \\ &+\frac{1}{2}M_3(\dot{x}_b+\dot{x}_c+h_3(\dot{\theta}_b+\dot{\theta}_c)+\dot{x}_o+\dot{x}_3)^2 + \frac{1}{2}M_4(\dot{x}_b+\dot{x}_c+h_4(\dot{\theta}_b+\dot{\theta}_c)+\dot{x}_o+\dot{x}_4)^2 \end{aligned} \tag{8}$$

$$\begin{aligned} V = &\frac{1}{2}K_h x_c^2 + \frac{1}{2}K_{hr}x_c\theta_c + \frac{1}{2}K_r\theta_c^2 + \frac{1}{2}K_{rh}\theta_c x_c + \frac{1}{2}K_o x_o^2 + \frac{1}{2}K_1 x_1^2 + \frac{1}{2}K_2(x_2-x_1)^2 \\ &+\frac{1}{2}K_3(x_3-x_2)^2 + \frac{1}{2}K_4(x_4-x_3)^2 \end{aligned} \tag{9}$$

where M_c and J_c are the mass of the foundation and its moment of inertia, respectively, M_o, M_1, M_2, M_3, M_4 are the masses of the floor structure and h_o, h_1, h_2, h_3, h_4 the corresponding heights from the base foundation. Also, $K_h, K_r, K_{hr} = K_{rh}$ are the rigidities of the soil and K_o, K_1, K_2, K_3, K_4 inter-story stifnesses of the structure.

For a system with generalized coordinates $q_i = x_c, \theta_c, x_o, x_1, x_2, x_3, x_4$, the Lagrange equation of motion [11] are given by

$$\frac{d}{dt}\left(\frac{\partial T}{\partial \dot{q}_i}\right) + \frac{\partial V}{\partial q_i} = 0 \tag{10}$$

Applying Eq. 10 to Eqs. 8 and 9, equations of motion of the system are obtained. Doing this and adding the damping, the following matrix system of equations are obtained:

$$\boldsymbol{M}_s\ddot{\boldsymbol{U}}_s(t) + \boldsymbol{C}_s\dot{\boldsymbol{U}}_s(t) + \boldsymbol{K}_s\boldsymbol{U}_s(t) = -\boldsymbol{M}_s\left\{\boldsymbol{s}_x\ddot{x}_b(t) + \boldsymbol{s}_\theta\ddot{\theta}_b(t)\right\} \tag{11}$$

where $\mathbf{U}_s = \{\mathbf{X}_e^T, x_o, x_c, \theta_c\}^T$ is the displacement vector of the system, being $\mathbf{X}_e^T = \{x_4, x_3, x_2, x_1\}$, $\mathbf{s}_x = \{\mathbf{0}^T, 1, 0\}^T$ and $\mathbf{s}_\theta = \{\mathbf{0}^T, 0, 1\}^T$. In addition, $\mathbf{M}_s$, $\mathbf{C}_s$ and $\mathbf{K}_s$ are the matrices of mass, damping and stiffness of the system, assembled as follows:

$$\boldsymbol{M}_s = \left[\begin{array}{c|ccc} \boldsymbol{M}_e & \boldsymbol{M}_e\boldsymbol{l}_x & \boldsymbol{M}_e\boldsymbol{l}_x & \boldsymbol{M}_e\boldsymbol{l}_\theta \\ \hline \boldsymbol{l}_x^T\boldsymbol{M}_e & M_o + \boldsymbol{l}_x^T\boldsymbol{M}_e\boldsymbol{l}_x & M_o + \boldsymbol{l}_x^T\boldsymbol{M}_e\boldsymbol{l}_x & M_o h_o + \boldsymbol{l}_x^T\boldsymbol{M}_e\boldsymbol{l}_\theta \\ \boldsymbol{l}_x^T\boldsymbol{M}_e & M_o + \boldsymbol{l}_x^T\boldsymbol{M}_e\boldsymbol{l}_x & M_c + M_o + \boldsymbol{l}_x^T\boldsymbol{M}_e\boldsymbol{l}_x & M_o h_o + \boldsymbol{l}_x^T\boldsymbol{M}_e\boldsymbol{l}_\theta \\ \boldsymbol{l}_\theta^T\boldsymbol{M}_e & M_o h_o + \boldsymbol{l}_\theta^T\boldsymbol{M}_e\boldsymbol{l}_x & M_o h_o + \boldsymbol{l}_\theta^T\boldsymbol{M}_e\boldsymbol{l}_x & J_c + M_o h_o^2 + \boldsymbol{l}_\theta^T\boldsymbol{M}_e\boldsymbol{l}_\theta \end{array}\right] \tag{12}$$

$$\boldsymbol{C}_s = \left[\begin{array}{c|ccc} \boldsymbol{C}_e & \mathbf{0} & \mathbf{0} & \mathbf{0} \\ \hline \mathbf{0}^T & C_o & 0 & 0 \\ \mathbf{0}^T & 0 & C_h & C_{hr} \\ \mathbf{0}^T & 0 & C_{rh} & C_r \end{array}\right] \tag{13}$$

$$K_s = \left[\begin{array}{c|ccc} \boldsymbol{K}_e & \mathbf{0} & \mathbf{0} & \mathbf{0} \\ \hline \mathbf{0}^T & K_o & 0 & 0 \\ \mathbf{0}^T & 0 & K_h & K_{hr} \\ \mathbf{0}^T & 0 & K_{rh} & K_r \end{array}\right] \tag{14}$$

where $\boldsymbol{l}_x = \{1, 1, 1, 1\}^T$ and $\boldsymbol{l}_\theta = \{h_4, h_3, h_2, h_1\}^T$ are vectors of coefficients of influence of the excitation. Also $\boldsymbol{M}_e$ and $\boldsymbol{K}_e$ are the mass and stiffness matrices of the fixed-base structure, given by

$$\boldsymbol{M}_e = \begin{bmatrix} M_4 & 0 & 0 & 0 \\ 0 & M_3 & 0 & 0 \\ 0 & 0 & M_2 & 0 \\ 0 & 0 & 0 & M_1 \end{bmatrix} \tag{15}$$

$$\boldsymbol{K}_e = \begin{bmatrix} K_4 & -K_4 & 0 & 0 \\ -K_4 & K_3 + K_4 & -K_3 & 0 \\ 0 & -K_3 & K_2 + K_3 & -K_2 \\ 0 & 0 & -K_2 & K_1 + K_2 \end{bmatrix} \tag{16}$$

To characterize the isolation system, it is necessary to introduce the following two parameters:

$$T_o = \frac{2\pi}{\omega_o} \quad \text{with} \quad \omega_o = \sqrt{\frac{k_o}{M_o + \sum_{n=1}^{4} M_n}} \tag{17}$$

$$\zeta_o = \frac{C_o}{2\left(M_o + \sum_{n=1}^{4} M_n\right)\omega_o} \tag{18}$$

where T_o is interpreted as the natural period ζ_o as the damping ratio of the isolation system with the structure assumed rigid.

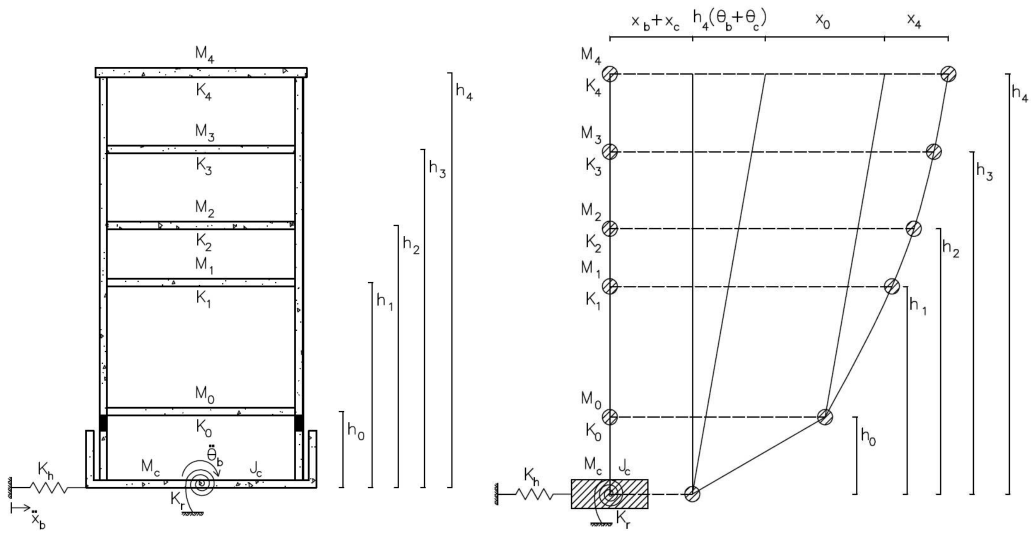

Fig. 4. (Left) Reference model for soil-structure systems with seismic isolation.
(Right) Deformed configuration of the soil-isolator-structure system.

5.3 Consideration of damping

To construct the damping matrix, it is assumed that the fixed-base structure has classical modes of vibration. This idealization is appropriate when the damping is uniformly distributed throughout the structure. So, damping ratios can be assigned to fixed-base natural modes and thus determine the damping matrix.

To construct a classical damping matrix from modal damping ratios, first natural frequencies ω_n and mode shapes matrix $\boldsymbol{\Phi}_e = [\boldsymbol{\Phi}_1, \boldsymbol{\Phi}_2, \boldsymbol{\Phi}_3, \boldsymbol{\Phi}_4]$ must be calculated solving the problem of eigenvalues

$$\left[\boldsymbol{K}_e - \omega_n^2 \boldsymbol{M}_e\right]\boldsymbol{\Phi}_n = \boldsymbol{0} \tag{19}$$

for the undamped structure. If the modes are normalized with respect to the mass such that

$$\boldsymbol{\Phi}_e^T \boldsymbol{M}_e \boldsymbol{\Phi}_e = \boldsymbol{I} = \begin{bmatrix} 1 & 0 & 0 & 0 \\ 0 & 1 & 0 & 0 \\ 0 & 0 & 1 & 0 \\ 0 & 0 & 0 & 1 \end{bmatrix} \tag{20}$$

then, it must be

$$\boldsymbol{\Phi}_e^T \boldsymbol{C}_e \boldsymbol{\Phi}_e = \boldsymbol{\zeta}_e = \begin{bmatrix} 2\zeta_1\omega_1 & 0 & 0 & 0 \\ 0 & 2\zeta_2\omega_2 & 0 & 0 \\ 0 & 0 & 2\zeta_3\omega_3 & 0 \\ 0 & 0 & 0 & 2\zeta_4\omega_4 \end{bmatrix} \tag{21}$$

From here, the damping matrix is deduced as

$$\boldsymbol{C}_e = [\boldsymbol{\Phi}_e^T]^{-1} \boldsymbol{\zeta}_e [\boldsymbol{\Phi}_e]^{-1} \tag{22}$$

The damping ratios ζ_n are reasonably assigned to each mode depending on the characteristics of the structure. Here, 5% damping for all modes is considered. The computation of the damping matrix can be improved by using the orthogonality relation given by Eq. 20. Specifically, it can be seen that

$$[\boldsymbol{\Phi}_e]^{-1} = \boldsymbol{\Phi}_e^T \boldsymbol{M}_e \tag{23}$$

$$[\boldsymbol{\Phi}_e^T]^{-1} = \boldsymbol{M}_e \boldsymbol{\Phi}_e \tag{24}$$

Substituting Eqs. 23 and 24 in Eq. 22, it is has

$$\boldsymbol{C}_e = \boldsymbol{M}_e [\boldsymbol{\Phi}_e \boldsymbol{\zeta}_e \boldsymbol{\Phi}_e^T] \boldsymbol{M}_e \tag{25}$$

In terms of modal superposition, Eq. 25 is expressed as

$$\boldsymbol{C}_e = \boldsymbol{M}_e \left(\sum_{n=1}^{4} 2\zeta_n \omega_n [\boldsymbol{\phi}_n \boldsymbol{\phi}_n^T] \right) \boldsymbol{M}_e \tag{26}$$

Each term of the sum represents the contribution of the n-th modal damping of the damping matrix. The contribution of the higher modes of vibration can be neglected without numerical problems.

5.4 System Response

To determine the response of the system is convenient to use the method of the complex frequency response [11]. Thus, natural frequencies of the system and amplitudes of vibration of the considered degrees of freedom, can be simultaneously computed. Applying the Fourier transform in both sides of Eq. 11, it is has that

$$\left[\boldsymbol{K}_s + i\omega \boldsymbol{C}_s - \omega^2 \boldsymbol{M}_s \right] \boldsymbol{U}_s(\omega) = -\ddot{x}_g(\omega) \boldsymbol{M}_s \left\{ \boldsymbol{s}_x H_x(\omega) + \boldsymbol{s}_\theta H_\theta(\omega) \right\} \tag{27}$$

where $\boldsymbol{U}_s(\omega)$ and $\ddot{x}_g(\omega)$ represent the Fourier transformed of the system response and the excitation on the surface, respectively. Solving Eq. 27 it is obtained the response of the system in the frequency domain, from which the corresponding response can be determined in the time domain through Fourier's synthesis.

Identifying the frequencies of the fixed base structure is possible by the transfer function of the roof

$$H_e(\omega) = \frac{x_b + x_c + h_4(\theta_b + \theta_c) + x_o + x_4}{x_g} \tag{28}$$

For the computation of floor spectra, it is necessary to determine the transfer function of the base

$$H_o(\omega) = \frac{x_b + x_c + h_o(\theta_b + \theta_c) + x_o}{x_g} \tag{29}$$

These complex functions relate the roof or base-structure responses with the excitation on the ground surface.

6 RESULTS FOR THE STUDIED CASE

For the SSI analysis, the structural model SF6 was used (shown in fig 5), properly stiffnessed with perimetral chevron braced to avoid the presence of a soft first floor. This is the model for the building with fixed base, without considering base isolators and supporting soil.

Table 1 contains weights and heights of each floor, as well as inter-story stiffnesses in two orthogonal directions. On the other hand, x direction corresponds to the rigid side, with fundamental period $T_x = 0.5$ s, and y direction corresponds to the flexible one, with fundamental period $T_y = 0.6$ s. The weight of the isolated structure is $W_o = 833.29$ t. The stiffness of the system for a period $T_o = 3.5$ s is $K_o = 4\pi^2 W_o / g T_o^2 = 2.74$ t/cm. The foundation is a rectangular slab of 20.1 m length, 13.80 m width and 3.5 m depth.

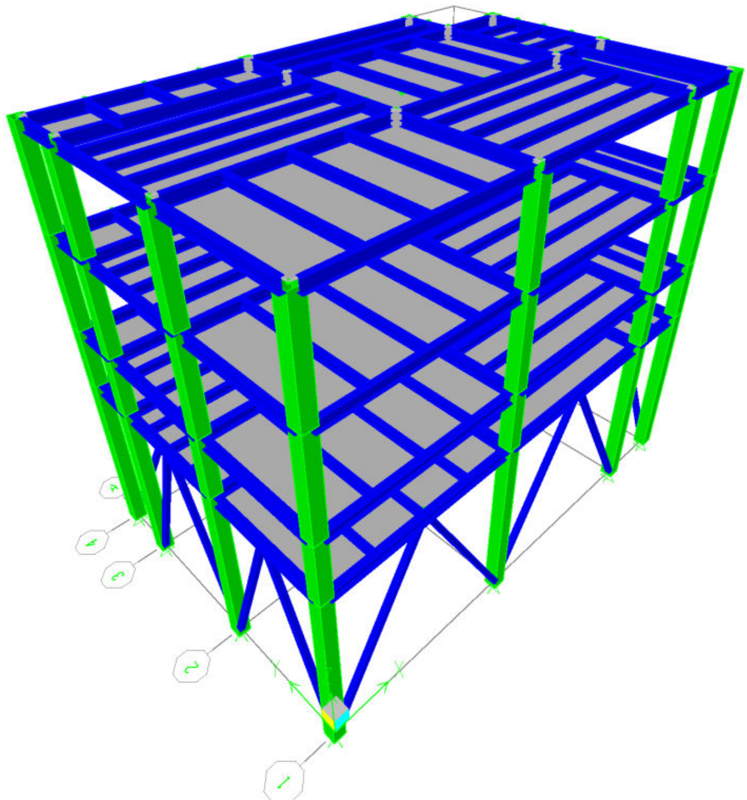

Fig. 5. Model of the SF6 building with fixed base

Level	W (t)	h (m)	Kx (t/cm)	Ky (t/cm)
4	134.79	20.90	79.61	60.41
3	141.66	17.10	119.20	93.84
2	142.75	13.30	298.24	221.61
1	160.25	10.80	219.70	120.52
0	253.84	3.5	2.74	2.74
Base	330.97		Variable	Variable

Table 1. Parameters of the SF6 building isolated at its base

6.1 Transfer functions

Transfer functions allows to simultaneosly identify natural frequencies of the system and amplitudes of vibration of the degrees of freedom. Fig. 6 shows roof transfer functions for the structure with fixed-base ($K_o = \infty$ and $V_s = \infty$) and for the isolated structure without and with SSI effects. Computations were done for the two directions of analysis, considering the damping factors $\zeta_o = 5$ and 15% for the isolation system.

Transfer functions that show major amplifications are the ones corresponding to the fixed-base structure, while functions that show minor amplification are the ones corresponding to the isolated structure without SSI. The SSI effects are little significant in high frecuencies, near to the frequencies of the structure with fixed base. Dynamic decoupling between the isolation period and the fundamental period of the structure grows when SSI is considered, such that the seismic isolation continues to be effective.

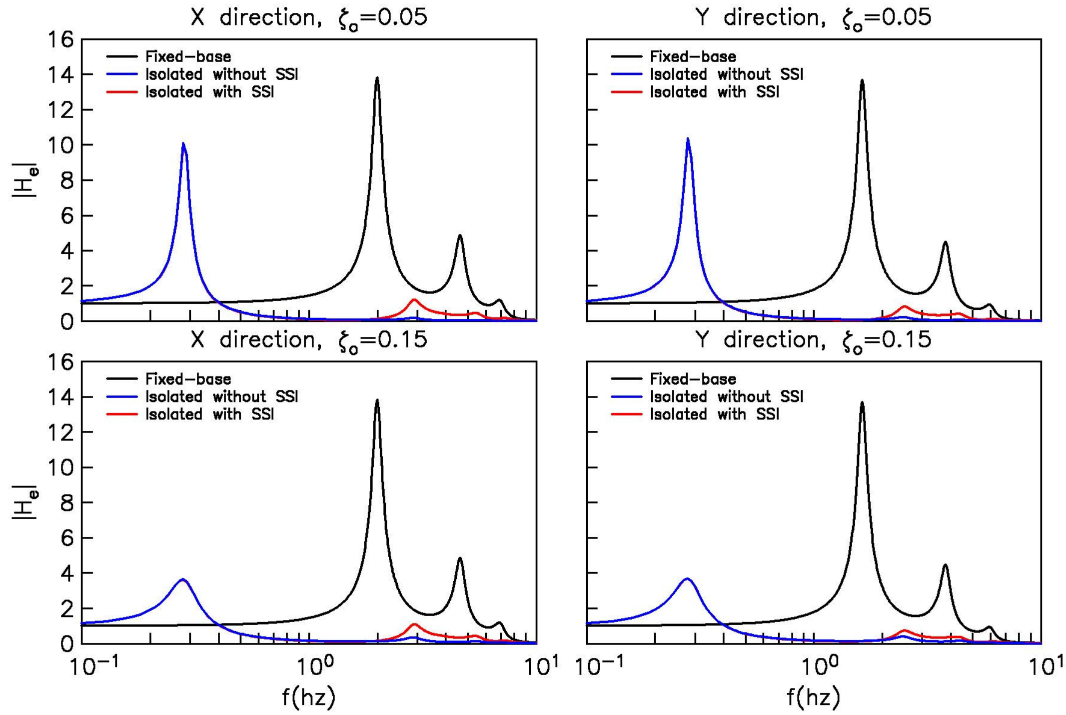

Fig. 6. Roof transfer functions for the fixed-base structure (black) and for the isolated structure without (blue) and with (red) SSI, Narvarte site.

6.2 Displacements and shear forces distribution

To determine the time response under seismic excitation, convolution of the system transfer functions with design simulated earthquakes were done. Average values of peak shear forces and displacements for the fixed-base structure and the isolated structure without and with SSI were computed.

Fig. 7 shows shear force and lateral displacement distributions from the roof to the base foundation, for the fixed-base structure ($K_o = \infty$ and $V_s = \infty$) and for the isolated structure without and with SSI. Calculations were done for the two directions of analysis, considering damping ratios $\zeta_o = 5$ and 15% for the isolation system.

The SSI effects in the shear force are relatively more important than in the displacement, especially in the superior floors. The effectiveness of the isolation, when SSI is accounted for, is preserved even for low damping ratio. The relative displacements of the structure, behaved as rigid body, become insignificant when compared with the deformations of the isolators, which are less than 30 cm for 5% damping.

It should be noted that the computation of seismic forces and lateral displacements for the design earthquake, was done disregarding the inelastic behavior of the base isolators. Contrarily, the non linear behavior of the supporting soil was accounted for.

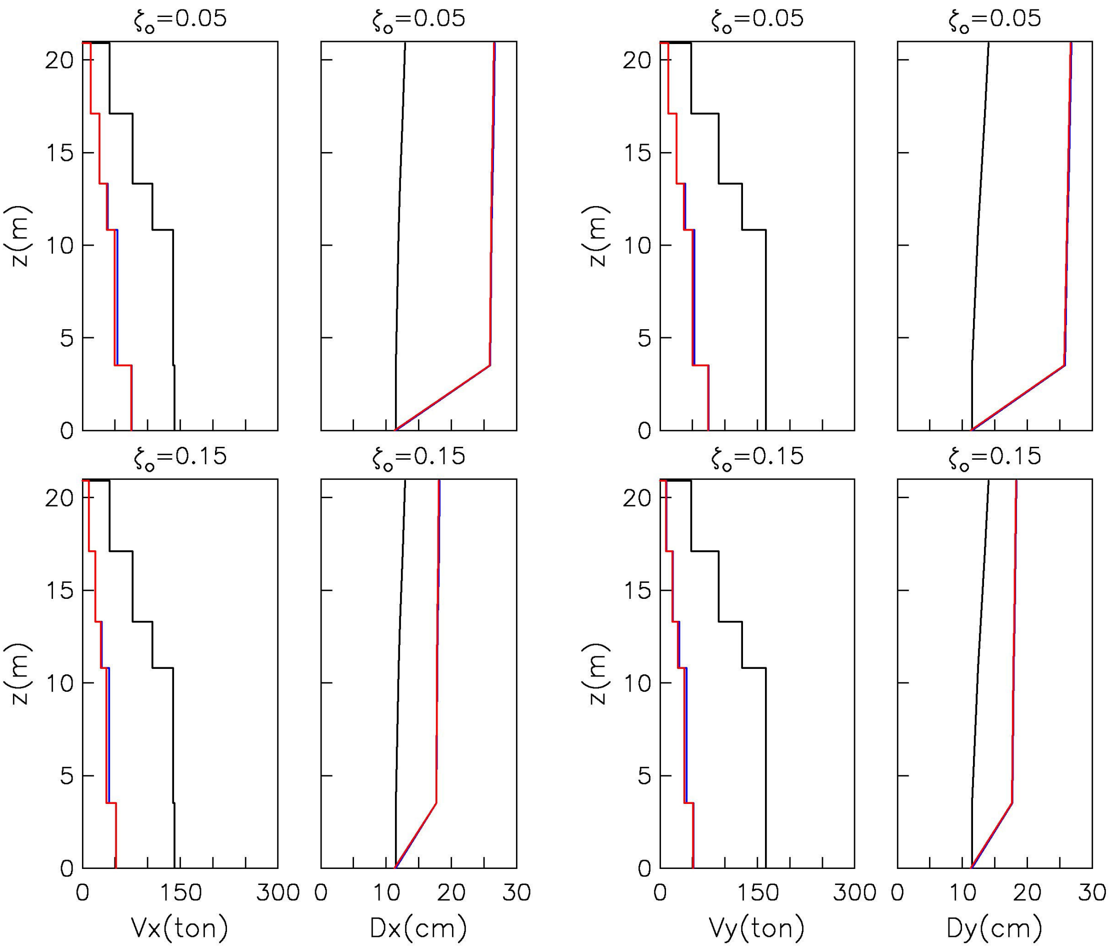

Fig. 7. Variations of shear force and displacement with the heihght for the fixed-base structure (black) and for the isolated structure without (blue) and with (red) SSI. Narvarte site.

6.3 Floor spectra

Floor spectra represent the easiest way to estimate SSI effects in the effectiveness of the isolation. Fig. 8 shows such spectra for the isolated structure without and with SSI effects, compared with the free-field spectrum. Computations were done for both directions of analysis, considering damping ratios $\zeta_o = 5$ and 15% for the isolation system. Changes on response spectra in short periods are due to the SSI effects, being kinematic effects more important than inertial effects. These results show that smaller seismic forces are developed in the structure-isolator system (without SSI) than in the structure-isolator-soil system (with SSI), although SSI effects are relevant only in short periods. Additionally, it is shown that the effectiveness of the isolation is notably increased for 15% damping.

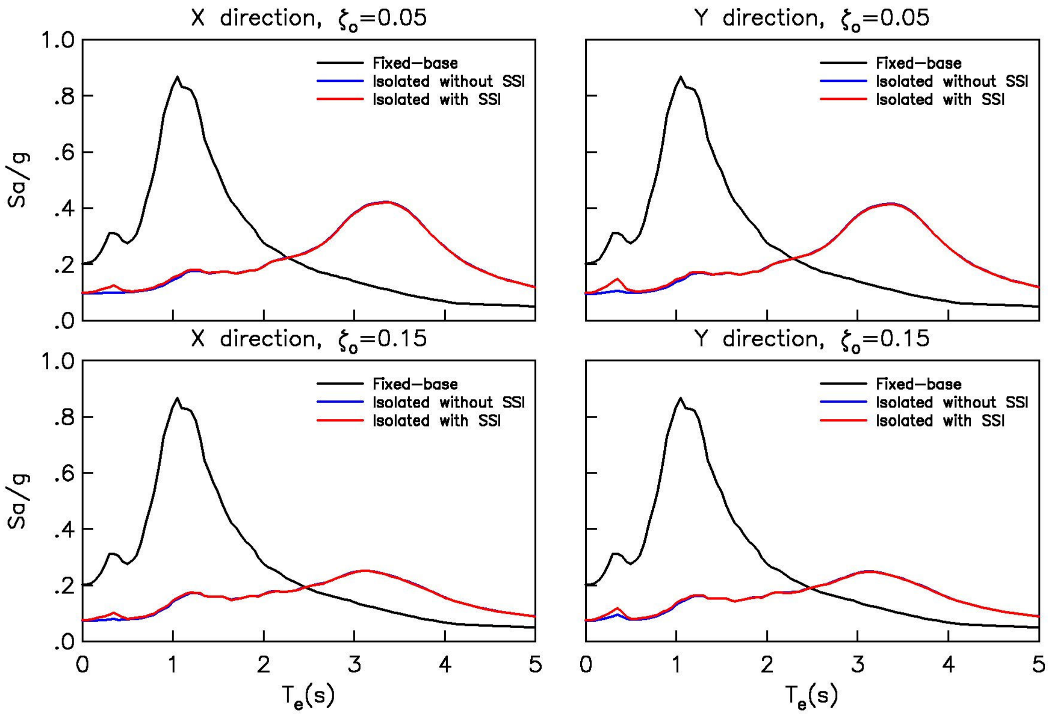

Fig. 8. Response spectra for the fixed-base structure (black)
and for the isolated structure without (blue) and with (red) SSI. Narvarte site.

7 CONCLUSIONS

- The aim of this study was to evaluate the feasibility of using seismic isolation in buildings for encapsulated substations in the Valley of Mexico. To do that, it was necessary to consider the effects of SSI (kinematic and inertial) in the model of analysis.
- Seismic excitation was given in terms of a uniform hazard spectrum (UHS) at rock for 475 year return period.
- The studied site, called Narvarte, is near 1 s period, and 40 m depth basement.
- Frequencies identification of the fixed base structure was done by using the transfer function of the roof. For the computation of floor spectra, the transfer function of the base was used.

- Transfer functions that show major amplifications are the ones corresponding to the fixed-base structure, while functions that show minor amplification are the ones corresponding to the isolated structure without SSI. The SSI effects are little significant in high frequencies, near to the frequencies of the structure with fixed base.
- SSI effects in the shear force are relatively more important than in the displacement, especially in the superior floors. The effectiveness of the isolation, when SSI is accounted for, is preserved even for low damping ratio. The relative displacements of the structure, behaved as rigid body, become insignificant when compared with the deformations of the isolators, which are less than 30 cm for 5% damping.
- Results show that smaller seismic forces are developed in the structure-isolator system (without SSI) than in the structure-isolator-soil system (with SSI), although SSI effects are relevant only in short periods. Additionally, it is shown that the effectiveness of the isolation is notably increased for 15% damping.

REFERENCES

[1] A. S. Veletsos, Design concepts for dynamics of soil-structure interaction, Eds. P Gülkan and R W Clough, Kluwer Academic Publishers, 1993.

[2] E. Kausel, R. V. Whitman, J. P. Morray and F. Elsabee, The spring method for embedded foundations, *Nuclear Engineering and Design*, Vol. 48, 1978.

[3] N. A. Haskell, Crustal reflection of plane P and SV waves, *Journal of Geophysical Research*, Vol. 67, 1962.

[4] M. Ordaz, E. Miranda and J. Avilés, Propuesta de espectros de diseño por sismo para la ciudad de México, *Ingeniería de Estructuras*, Vol. 8, 2003.

[5] NTCDS-RCDF (2004), Normas Técnicas Complementarias para Diseño por Sismo, *Reglamento de Construcciones para el Distrito Federal*, Gaceta Oficial del Departamento del Distrito Federal.

[6] H. B. Seed and I. M. Idriss, Influence of soil conditions on ground motions during earthquakes, *Journal of the Soil Mechanics and Foundation Division*, ASCE, Vol. 95, 1969.

[7] M. Iguchi, An approximate analysis of input motions for rigid embedded foundations, *Transactions of Architectural Institute of Japan*, No. 315, 1982.

[8] G. Gazetas, Analysis of machine foundation vibrations: state of the art, *Soil Dynamics and Earthquake Engineering*, Vol. 2, 1983.

[9] J. L. Tassoulas J L and E Kausel, Elements for the numerical analysis of wave motion in layered strata, *Journal of Numerical Methods in Engineering*, Vol. 19, 1983.

[10] E. Kausel, Program SUPELM Ver. 2.0, Foundations Embedded in Layered Media: Dynamic Stiffnesses and Response to Seismic Waves, 1992.

[11] R. W. Clough and J. Penzien, *Dynamics of Structures*, McGraw-Hill, 1975.